

SCIENTIFIC REPORTS



OPEN

Single-photon emission of two-level system via rapid adiabatic passage

Qiang Miao & Yujun Zheng

Received: 06 July 2016

Accepted: 16 August 2016

Published: 07 September 2016

In this paper, we present a high quality single-photon source based on the two-level system undergoing rapid adiabatic passage (RAP). A trigger strategy (sweet region) is suggested to optimize the single-photon emission and explain a counter-intuitive phenomenon on the optimal parameters. The RAP strategy of single-photon source is robust against control error and environmental fluctuation.

Single-photons generated “on demand” have evoked the interests of physicists over the last decades, not only for the improvement in recognition of photon itself, but also for the requirements of explosive-growing quantum information process (QIP)¹. Also, the high quality single-photon source plays an important role in some applications, such as truly random numbers generation², linear-optics quantum computation³, quantum cryptography, or more precisely, quantum key distribution (QKD)^{4,5}, etc. Therefore, a resilient and deterministic single-photon source is of great benefit to develop building block in QIP.

Two-level system (TLS) has been widely employed to be used as single-photon sources. A popular route is employing the resonance pulses with fixed area, namely, a “ π -pulse” is chosen to drive vector state to flip into excited state accurately^{6,7}. This scheme can be fast, but it is sensitive to control parameters. Alternatively, in this work, we present a triggered single-photon source based on the TLS undergoing the rapid adiabatic passage (RAP) scheme in theoretical frame. In this case, the TLS interacts with a nearly resonance driving field, and a time-dependent detuning between driving field and inner system is needed to sweep around the level-crossing, which could be made by the Stark-chirped pulse^{8,9} or an radio-frequency field¹⁰.

In this work, the nature of single-photon emission of TLS based on the RAP scheme is investigated by employing the photon counting statistics of generating function^{11–18}. For the case that TLS undergoes the RAP, the time-dependent detuning is modulated periodically to trigger sequential photon emissions. We illustrate the ladder features in few emitted photons $\langle N \rangle$ and the big negative value of the Mandel’s Q parameter in the photon trigger events. By means of Landau-Zener (LZ) formula^{19–22}, we analyze the single-photon emission and propose the trigger strategy of RAP for the first time. By this trigger strategy, the quality of single-photon emission can, avoiding the tedious analysis, be improved simply and explicitly. This optimal strategy succeeds in explaining a counter-intuitive result. That is, under certain constraint of control parameter, the faster trigger frequency leads to better single-photon emission. Besides, this strategy of triggered single-photon source shows more resilience against control errors and environmental fluctuations than resonance pulse method.

TLS Model

The Hamiltonian of the TLS can be described by²³

$$H = -\frac{1}{2}\varepsilon(t)\sigma_z - \frac{1}{2}\Delta\sigma_x, \quad (1)$$

where $\varepsilon(t)$ is the time-dependent detuning, Δ is the coupling strength between the ground state $|g\rangle$ and excited state $|e\rangle$. σ_x and σ_z are the Pauli matrices and we set $\hbar = 1$ throughout this manuscript. In this work, we consider the case that $\varepsilon(t)$ is modulated via²³

$$\varepsilon(t) = \varepsilon_0 + A \cos(\omega t), \quad (2)$$

where A is modulation amplitude, ω denotes modulation frequency and ε_0 represents static detuning, respectively.

School of Physics, Shandong University, Jinan 250100, China. Correspondence and requests for materials should be addressed to Y.Z. (email: yzheng@sdu.edu.cn)

Photon counting statistics via Generating Functions formula

The time evolution of density matrix $\rho(t)$ of single quantum system obeys the Liouville-von Neumann equation,

$$\frac{\partial}{\partial t}\rho(t) = -i[\mathcal{H}, \rho(t)] + \mathcal{L}\rho(t), \quad (3)$$

where \mathcal{L} is the superoperator including the spontaneous emission rate Γ which is caused by the vacuum fluctuation.

The generating function approach for counting spontaneous photon emission events is proposed, and employed to investigate different questions^{11–18,24–29}. The generating function is defined as following^{11–13}

$$\mathcal{G}_{ij}(s, t) = \sum_n \rho_{ij}^{(n)} s^n, \quad (4)$$

where $\rho_{ij}^{(n)}$ ($i, j = e, g$) represents the portion of density matrix corresponding to that n photons have been spontaneously emitted in the time interval $[0, t]$. And, s is an auxiliary parameter counting the photon emission events.

By employing the generalized Bloch vector notation^{11–13},

$$\begin{aligned} \mathcal{U}(s, t) &\equiv \frac{1}{2}(\mathcal{G}_{eg} + \mathcal{G}_{ge}), \quad \mathcal{V}(s, t) \equiv \frac{1}{2i}(\mathcal{G}_{eg} - \mathcal{G}_{ge}), \\ \mathcal{W}(s, t) &\equiv \frac{1}{2}(\mathcal{G}_{gg} - \mathcal{G}_{ee}), \quad \mathcal{Y}(s, t) \equiv \frac{1}{2}(\mathcal{G}_{gg} + \mathcal{G}_{ee}), \end{aligned} \quad (5)$$

the generating function equations can, by employing Eqs 3, 4 and 5, be written as

$$\frac{\partial}{\partial t}\mathbb{Y}(s, t) = \mathbb{M}(s, t)\mathbb{Y}(s, t), \quad (6)$$

where $\mathbb{Y}(s, t) = (\mathcal{U}(s, t), \mathcal{V}(s, t), \mathcal{W}(s, t), \mathcal{Y}(s, t))^{\dagger}$ and $\mathbb{M}(s, t)$ are given by

$$\mathbb{M}(s, t) = \begin{pmatrix} -\frac{\Gamma}{2} & \varepsilon(t) & 0 & 0 \\ -\varepsilon(t) & -\frac{\Gamma}{2} & \Delta & 0 \\ 0 & -\Delta & -\frac{\Gamma}{2}(1+s) & \frac{\Gamma}{2}(1+s) \\ 0 & 0 & \frac{\Gamma}{2}(1-s) & -\frac{\Gamma}{2}(1-s) \end{pmatrix}. \quad (7)$$

The probabilities of emitted n photons in time interval $[0, t]$ can be extracted from $2\mathcal{Y}(s, t)$ as follows^{11–13}

$$p_n(t) = \frac{2}{n!} \frac{\partial^n}{\partial s^n} \mathcal{Y}(s, t) \Big|_{s=0}. \quad (8)$$

The factorial moments of photon emission can be simply obtained by taking derivatives with respect to s evaluated at $s=1$ ^{11–13}, namely

$$\begin{aligned} \langle N^{(r)} \rangle(t) &\equiv \langle N(N-1)(N-2)\cdots(N-r+1) \rangle \\ &= 2 \frac{\partial^r}{\partial s^r} \mathcal{Y}(s, t) \Big|_{s=1}. \end{aligned} \quad (9)$$

Thereinto, the average photon emission number $\langle N \rangle = \langle N^{(1)} \rangle$ is given by $r=1$ (the first factorial moment). Meanwhile, the Mandel's Q parameter

$$Q = \frac{\langle N^{(2)} \rangle - \langle N^{(1)} \rangle^2}{\langle N^{(1)} \rangle}, \quad (10)$$

follows immediately, which characterizes the statistical properties of emitted photons. The case of $Q < 0$ is called sub-Poissonian distribution (anti-bunching behavior) and $Q > 0$ is named super-Poissonian distribution (bunching behavior). Particularly, a perfect single-photon emission results in $Q = -1$.

Single-photon emission via trigger strategy of RAP

Based on the photon counting statistics of generating function approach, one can study the properties of photon emission from TLS undergoing level-crossing. Before giving the quantitative results, we analyze the RAP strategy of single-photon emission and its optimal control region by LZ formula.

Supposing that TLS is initialized at its ground state $|g\rangle$, the detuning sweeps with a finite velocity v and passes through level-crossing. The population inversion occurs in the vicinity of level-crossing, and the asymptotic excited state population $P_{g \rightarrow e}$ is, from LZ formula, given by

$$P_{g \rightarrow e} = P_{LZ} = 1 - \exp(-2\pi\delta), \quad (11)$$

where the adiabaticity parameter

$$\delta = \frac{\Delta^2}{4\nu}, \quad (12)$$

divides LZ problem into two regimes: non-adiabatic passage with $\delta \ll 1$ and near-adiabatic passage with $\delta \gtrsim 1$. In this work, we focus on the near-adiabatic passage to generate near-complete population inversion, which is crucial to trigger single-photon emission.

Considering the harmonic sweeping, the sweep velocity in level-crossing vicinity is given by²³

$$\nu = A\omega \sqrt{1 - \left(\frac{\varepsilon_0}{A}\right)^2}. \quad (13)$$

One can, by using Eqs 12 and 13, distinguish between the non-adiabatic passage $A\omega \gg \Delta^2$ and the near-adiabatic passage $A\omega \leq \Delta^2$. In addition, the time t_{LZ} of LZ transition measures the population inversion speed. t_{LZ} , as an important parameter in LZ transition, is given by²³

$$t_{LZ} \sim \frac{1}{\sqrt{\nu}} \max(1, \sqrt{\delta}) \sim \begin{cases} \frac{\Delta}{2\nu} & \nu < \frac{\Delta^2}{4}, \\ \frac{1}{\sqrt{\nu}} & \nu \geq \frac{\Delta^2}{4}. \end{cases} \quad (14)$$

Eq. 14 means that t_{LZ} is a monotonically decreasing function of ν .

At each level-crossing vicinity, the ground state $|g\rangle$ is triggered to excited state $|e\rangle$ in near-adiabatic regime. Whereafter, $|e\rangle$ will emit a photon due to spontaneous emission rate Γ , and go back to $|g\rangle$ before next trigger event. The cyclic repeats will construct a sequential photon-emitter with trigger frequency 2ω . To present good quality single-photon emission, the population inversion should approach unit for each passage event. Meanwhile, the inversion time should be short to minimize the effect of Γ . This control condition can be noted as rapid and adiabatic passage. Namely,

(i) For adiabatic feature, from LZ formula of Eq. 11, it is necessary to slow down the sweep velocity ν to obtain near-complete inversion between $|g\rangle$ and $|e\rangle$.

(ii) For rapid feature, the time t_{LZ} of LZ transition should satisfy $t_{LZ} \cdot \Gamma \ll 1$ to protect LZ process against strong Γ .

This indicates that the above contradict requirements seek a sophisticated sweep velocity ν . Here we can notice as follows

$$\begin{aligned} \nu \sim \Delta^2 &\mapsto t_{LZ} \cdot \Delta \sim 1 \mapsto P_{g \rightarrow e} \sim 0.792, \\ \nu \sim \frac{1}{2}\Delta^2 &\mapsto t_{LZ} \cdot \Delta \sim \sqrt{2} \mapsto P_{g \rightarrow e} \sim 0.957, \\ \nu \sim \frac{1}{4}\Delta^2 &\mapsto t_{LZ} \cdot \Delta \sim 2 \mapsto P_{g \rightarrow e} \sim 0.998. \end{aligned}$$

The first one gives the boundary of adiabatic feature, as faster ν will lead to incomplete inversion. And the last one gives the boundary of rapid feature, as lower ν or longer t_{LZ} makes no significant improvement in population inversion. Based on the above analysis, the optimal control region is suggested as follows

$$\Delta^2/4 < \nu < \Delta^2, \quad (15)$$

to ensure rapid and adiabatic feature, and we mark Eq. 15 as the *sweet region*. In this paper, the sweet region plays a central role in analyzing single-photon emission. Also, in this region, $t_{LZ} \cdot \Delta$ gives the same order of sequential pulses control with π -pulse. Meanwhile, $\Delta \gg \Gamma$ is necessary to ensure population inversion in both RAP and π -pulse scheme.

In the following, we show the numerical results of single-photon emission via the photon counting statistics of the generating function formula, and verify the RAP strategy of single-photon generation in the sweet region.

Single-photon emission

Figure 1 shows the nature of few emitted photons. The left panel of the figure illustrates series of single-photon emission clearly. After each trigger event, the corresponding p_n dominates the dynamical process. Thereinto, $p_1 = 0.75$, $p_2 = 0.59$ and $p_3 = 0.48$ after each corresponding trigger events, respectively. In the inset of left panel, we can observe LZ transitions resulting from the sweep driving. However, due to effect of spontaneous radiation, the excited state collapses and the photon emission occurs between trigger events. The right panel of Fig. 1 shows that the Mandel's Q parameter drops down sharply at the beginning of LZ transition process and keeps big value negatively ($Q_{min} = -0.73$) during photon emission process. Significantly, the perfect ladder feature of single-photon emission is shown in $\langle N \rangle$ as noted in the inset of right panel of Fig. 1.

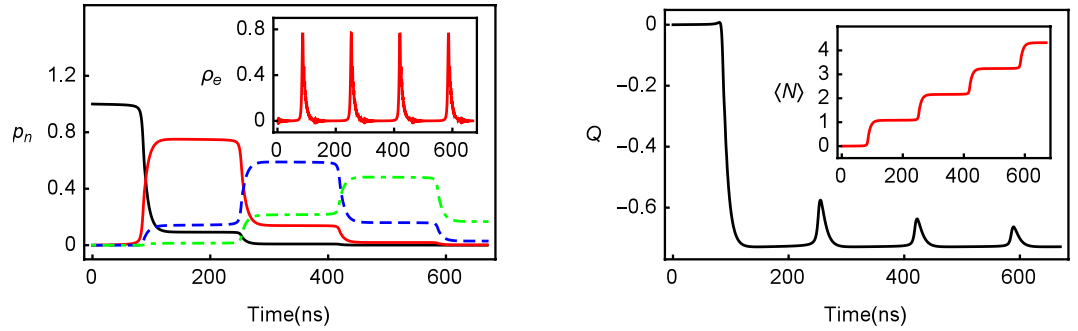


Figure 1. The results of photon counting statistics as a function of time t . In the left panel, p_n ($n=0, 1, 2, 3$) is the probabilities of n emitted photons. p_0 , p_1 and p_3 are presented by black solid lines, red solid lines, and blue dashed lines, respectively. In the inset, the population of excited state $|e\rangle$, ρ_e is shown. The right panel and its inset show the Mandel's Q parameter and average photon emission numbers $\langle N \rangle$ against time in unit of ns. The parameters, $\Gamma = 20$ MHz, $\Delta = 5\Gamma$, $\omega = 3$ MHz, and $\varepsilon_0 = 0$, were employed in the experiment of ref. 10. A is supposed to achieve better quality of single-photon emission with $A = 110\Gamma$.

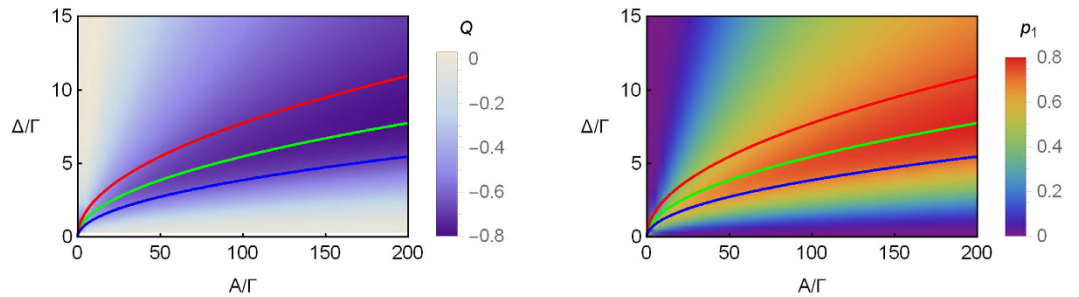


Figure 2. The distribution of the Mandel's Q parameter (left) and single-photon emission probability p_1 (right) after the first trigger event as function of A/Γ and Δ/Γ . In the panels, curves of $\nu = \Delta^2/4$, $\nu = \Delta^2/2$ and $\nu = \Delta^2$ are plotted by red, green and blue lines, respectively. One can find the best trace of single-photon emission mainly propagates along green lines. The parameters are $\Gamma = 20$ MHz, $\omega = 3$ MHz, and $\varepsilon_0 = 0$.

ω (MHz)	Q	p_0	p_1	p_2	Δ/Γ	A/Γ	ν/Δ^2
1	-0.70	0.06	0.71	0.20	4.2	200	0.57
3	-0.80	0.04	0.80	0.15	7.8	200	0.49
6	-0.84	0.03	0.84	0.12	11.7	200	0.44
12	-0.86	0.04	0.86	0.09	15	180	0.48

Table 1. The optimal single-photon emission of RAP in different modulation frequency ω^\dagger . ‡ The controlling parameter space is constrained by $A \leq 200\Gamma$ and $\Delta \leq 15\Gamma$. Other parameters are $\Gamma = 20$ MHz, and $\varepsilon_0 = 0$.

Verification about sweet region

Here, we show the high quality of single-photon emission can be obtained at the sweet region of Eq. 15.

Figure 2 shows the distribution of the Mandel's Q parameter (left) and single-photon emission probability (right) after the first trigger event. One can find the position of the high quality single-photon emission is located in the sweet region of Eq. 15, namely, $\Delta^2/4 < \nu = A\omega < \Delta^2$. That is, the region between red and blue lines in Fig. 2. Here, the best trace is along the curve of $\nu \sim \Delta^2/2$ (the green lines in the figure). Besides, along this sweet region, one can improve the quality of single-photon emission by increasing Δ . Obviously, the extremum of Q and p_1 is located in the end of sweet region.

Table 1 shows the typical values of Q , p_0 , p_1 and p_2 , and their optimal parameters under different modulation frequency ω . One can find the optimal locations perform as expectation: They follow a sophisticated sweep velocity ν around $\Delta^2/2$ and located in the end of sweet region. Noticeably, although small ω means that the interval between each trigger event is long enough to achieve distinguishable photon emission³⁰. However, Table 1 indicates a counter-intuitive result that smaller ω does not give the better single-photon emission. Actually, in the sweet region, Δ is limited by $\sqrt{A\omega}$. Such a small ω will lead to low Δ , which causes an inferior single-photon emission. To obtain the optimal modulation frequency, the sweet region should get the limitation of Δ ($\Delta = 15\Gamma$

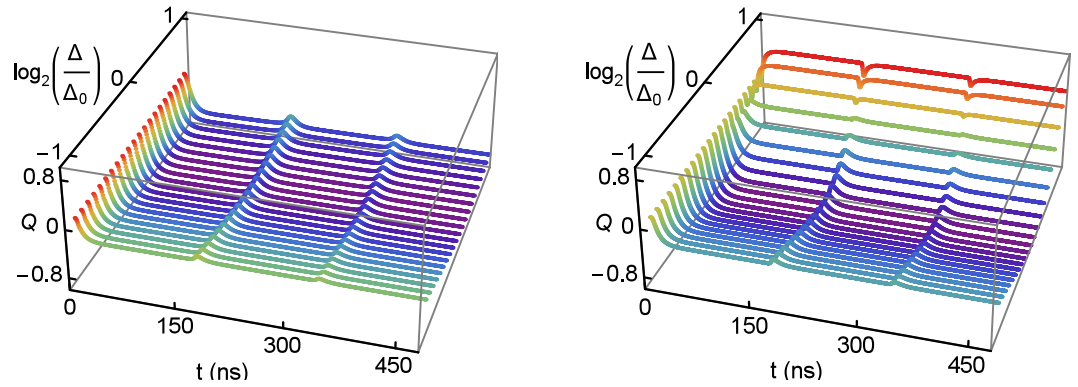


Figure 3. The time evolution of the Mandel's Q parameter as a function of $\log_2(\Delta/\Delta_0)$. The left panel is the result for RAP scheme, and the right panel is the result for the π -pulse scheme. The parameters are $\Gamma = 20$ MHz, $\Delta_0 = 5\Gamma$, $\varepsilon_0 = 0$, $A = 110\Gamma$, and $\omega = 3$ MHz.

Order	RAP					π -pulse				
	Q	$\langle N \rangle$	p_0	p_1	p_2	Q	$\langle N \rangle$	p_0	p_1	p_2
1	-0.69	1.06	0.12	0.72	0.14	-0.62	0.76	0.29	0.65	0.05
2	-0.69	2.11	0.01	0.17	0.55	-0.62	1.52	0.09	0.38	0.46
3	-0.69	3.16	0.00	0.03	0.21	-0.62	2.28	0.03	0.17	0.39

Table 2. The single-photon emission of RAP and π -pulse scheme[†]. [†]The data are extracted after each trigger events in the stable interval. The "Order" means the order of trigger events. One can find the Mandel's Q parameter remains stable and average photon emission number $\langle N \rangle$ jumps after each trigger event for both schemes. However, the RAP scheme shows a better quality of single-photon emission. The parameters are $\Gamma = 20$ MHz, $\Delta = 5\Gamma$, $A = 110\Gamma$, $\omega = 3$ MHz, $\varepsilon_- = 0$, $\varepsilon_+ = 5\Gamma$ and $R = 10$ MHz.

in Table 1) to reduce the impact of Γ . Meanwhile, the ω should be kept as small as possible to ensure distinguishable photon emission. As the expectation of our trigger strategy, we find when ω ranges from 9 to 13 (not shown in the table), the quality of single-photon emission is better than that of other modulation frequencies. Hence, the trigger strategy of sweet region by Eq. 15 can help optimizing the modulation frequency as well.

Besides, one can find that, in the sweet region, Q and p_1 show a quite smooth feature, especially along A/Γ . This feature implies that the RAP scheme is robust.

To analyze the robust features of single-photon emission based on RAP scheme, in the following, we compare the RAP and π -pulse schemes in the same laser coupling strength Δ and the same trigger frequency 2ω . In the π -pulse scheme, we turn off modulation of detuning and switch on and off laser field in fixed duration.

Control Error

As mentioned above, the RAP scheme is not sensitive to control parameter. However, in the π -pulse scheme, a fixed-area laser pulse is needed. The deviation of pulse strength will result in incomplete population inversion apparently. Here, we assume the optimal laser strength is defined by Δ_0 and study the deviation effect on single-photon emission, in which the deviation is measured by $\log_2(\Delta/\Delta_0)$.

Figure 3 shows the Mandel's Q parameter as a function of $\log_2(\Delta/\Delta_0)$ and time t for the RAP scheme (left) and the π -pulse scheme (right). Naturally, the optimal laser strength gives the minimal value of Q in both schemes. Noticeably, the deviation $\log_2(\Delta/\Delta_0)$ causes obvious change in the Mandel's Q parameter in the π -pulse scheme, as shown in the right panel of Fig. 3. Especially, the values of Q indicate that the emitted photons have a strong super-Poissonian distribution when $\Delta = 2\Delta_0$. In this case, the area of laser field is 2π rather than π , so that TLS is driven back to ground state $|g\rangle$ by laser pulse. Nevertheless, the RAP scheme shows its resilience against this error from laser strength (see the left panel of Fig. 3).

Spectral Diffusion Process

TLS may undergo perturbations from stochastic fluctuations of the surrounding. Here we employ the telegraph model of the surrounding to model the spectral diffusion, namely, the static detuning $\varepsilon_0(t)$ hops back and forth between two states ε_+ and ε_- with rate constant R in both directions^{11,12}. Based on the telegraphy model of the spectral diffusion, we have^{11,12}

$$\begin{pmatrix} \dot{\langle \hat{Y}_+(t) \rangle} \\ \dot{\langle \hat{Y}_-(t) \rangle} \end{pmatrix} = \begin{pmatrix} M_+ - R1 & R1 \\ R1 & M_- - R1 \end{pmatrix} \begin{pmatrix} \langle \hat{Y}_+(t) \rangle \\ \langle \hat{Y}_-(t) \rangle \end{pmatrix}, \quad (16)$$

where $\langle \mathbb{Y}(t) \rangle = \langle \mathbb{Y}_+(t) \rangle + \langle \mathbb{Y}_-(t) \rangle$, and \mathbb{Y}_\pm is the same with \mathbb{Y} in Eq. 6 but ε_0 is replaced by ε_\pm , respectively. The physical moments of photon counting statistics under the influences of the surrounding fluctuations can be extracted from Eq. 16.

Here we show the RAP scheme is also robust against spectral diffusion process but the π -pulse scheme isn't. Table 2 shows the photon emission statistics of the RAP and the π -pulse schemes for the same control parameters under spectral diffusion process. One can find the Mandel's Q parameter for the RAP scheme is bigger negatively than that for the π -pulse scheme. The accumulated average photon emission number $\langle N \rangle$ shows a high quality of single-photons feature for the former scheme. Specifically, in second trigger event, p_2 dominates the dynamics of the RAP scheme. As a comparison, p_1 makes a non-negligible contribution in the π -pulse scheme.

In conclusion, we present the RAP scheme to generate the high quality single-photon emission. The RAP scheme could trigger single-photons sequentially by periodical modulation of detuning. The sweet region, namely the optimal region of the single-photon emission has been suggested. To achieve better single-photon emission, the counter-intuitive modulation mode was given, which has been interpreted by our trigger strategy. Also, it has been shown that the RAP scheme is robust against control errors and spectral diffusion process.

References

- Bouwmeester, D., Ekert, A. & Zeilinger, A. *The Physics of Quantum Information* (Springer, 2000).
- Rarity, J. G. Quantum random-number generation and key sharing. *J. Mod. Opt.* **41**, 2435–2444 (1994).
- Knill, E., Laflamme, R. & Milburn, G. J. A scheme for efficient quantum computation with linear optics. *Nature* **409**, 46–52 (2001).
- Bennett, C. H. & Brassard, G. Quantum cryptography: Public key distribution and coin tossing. *Proc. IEEE Int. Conf. on Comp., Sys. and Sig. Proc. (Bangalore, India)* (1984).
- Bennett, C. H. & Brassard, G. Quantum public-key distribution system. *IBM Tech. Discl. Bull.* **28**, 3153–3163 (1985).
- Shen, Y. R. *The principles of nonlinear optics* (Wiley-Interscience, 2003).
- Zrenner, A. *et al.* Coherent properties of a two-level system based on a quantum-dot photodiode. *Nature* **418**, 612–614 (2002).
- Rickes, T. *et al.* Efficient adiabatic population transfer by two-photon excitation assisted by a laser-induced stark shift. *J. Chem. Phys.* **113**, 534–546 (2000).
- Yatsenko, L. P., Shore, B. W., Halfmann, T., Bergmann, K. & Vardi, A. Source of metastable $h(2s)$ atoms using the stark chirped rapid-adiabatic-passage technique. *Phys. Rev. A* **60**, R4237–R4240 (1999).
- Brunel, C., Lounis, B., Tamarat, P. & Orrit, M. Triggered source of single photons based on controlled single molecule fluorescence. *Phys. Rev. Lett.* **83**, 2722 (1999).
- Zheng, Y. & Brown, F. L. H. Single-molecule photon counting statistics via generalized optical Bloch equations. *Phys. Rev. Lett.* **90**, 238305 (2003).
- Zheng, Y. & Brown, F. L. Photon emission from driven single molecules. *J. Chem. Phys.* **119**, 11814–11828 (2003).
- Zheng, Y. & Brown, F. L. Single molecule photon emission statistics for non-Markovian blinking models. *J. Chem. Phys.* **121**, 3238–3252 (2004).
- Peng, Y., Zheng, Y. & Brown, F. L. Single molecule photon emission statistics of driven three-level systems. *J. Chem. Phys.* **126**, 104303 (2007).
- Peng, Y. & Zheng, Y. Photon statistics of v-type three-level system in single quantum dots. *Appl. Phys. Lett.* **92**, 092120 (2008).
- Peng, Y., Xie, S., Zheng, Y. & Brown, F. L. Single-molecule photon emission statistics for systems with explicit time dependence: Generating function approach. *J. Chem. Phys.* **131**, 214107 (2009).
- Peng, Y. & Zheng, Y. Photon emission from a single molecule in a solid matrix: Phase-delay control. *Phys. Rev. A* **88**, 013425 (2013).
- He, Y. & Dai, L. Reduction of single-photon emission from a single-emitter system by intersystem crossing. *Phys. Rev. A* **89**, 013839 (2014).
- Landau, L. D. On the theory of transfer of energy at collisions ii. *Phys. Z. Sowjetunion* **2**, 46–51 (1932).
- Zener, C. Non-adiabatic crossing of energy levels. *Proc. R. Soc. A* **137**, 696–702 (1932).
- Stückelberg, E. Theory of inelastic collisions between atoms (theory of inelastic collisions between atoms, using two simultaneous differential equations). *Helv. Phys. Acta* **5**, 369–422 (1932).
- Majorana, E. Atomi orientati in campo magnetico variabile. *Nuovo Cimento* **9**, 43–50 (1932).
- Shevchenko, S., Ashhab, S. & Nori, F. Landau–Zener–Stückelberg interferometry. *Physics Reports* **492**, 1–30 (2010).
- Wang, D. & Zheng, Y. Quantum interference in a four-level system of a rb^{87} atom: Effects of spontaneously generated coherence. *Phys. Rev. A* **83**, 013810 (2011).
- Zheng, Y. Comment on “coherent control of a v-type three-level system in a single quantum dot”. *Phys. Rev. Lett.* **101**, 049701 (2008).
- Peng, Y. & Zheng, Y. Coherent optical spectroscopy of a single quantum dot using photon counting statistics. *Phys. Rev. A* **80**, 043831 (2009).
- Miao, Q. & Zheng, Y. Coherent destruction of tunneling in two-level system driven across avoided crossing via photon statistics. *Sci. Rep.* **6**, 28959 (2016).
- Song, Z., Peng, Y., Sun, Z. & Zheng, Y. Spontaneously generated coherence in a rb atom via photon counting statistics. *Journal of Physics B: Atomic, Molecular and Optical Physics* **49**, 015001 (2016).
- Song, Z. & Zheng, Y. Radiative force on atoms from the view of photon emission. *Chin. Opt. Lett.* **13**, 042701 (2015).
- He, Y. & Barkai, E. Theory of single photon on demand from a single molecule source. *Phys. Chem. Chem. Phys.* **8**, 5056–5068 (2006).

Acknowledgements

This work was supported by the National Basic Research Program of China (973 Program, Grant No. 2015CB921004) and the National Science Foundation of China (Grant No. 11374191).

Author Contributions

Q.M. and Y.Z. made the theoretical analysis, Q.M. carried out numerical simulations and prepared the figures. All authors contributed to the manuscript writing.

Additional Information

Competing financial interests: The authors declare no competing financial interests.

How to cite this article: Miao, Q. and Zheng, Y. Single-photon emission of two-level system via rapid adiabatic passage. *Sci. Rep.* **6**, 32827; doi: 10.1038/srep32827 (2016).



This work is licensed under a Creative Commons Attribution 4.0 International License. The images or other third party material in this article are included in the article's Creative Commons license, unless indicated otherwise in the credit line; if the material is not included under the Creative Commons license, users will need to obtain permission from the license holder to reproduce the material. To view a copy of this license, visit <http://creativecommons.org/licenses/by/4.0/>

© The Author(s) 2016